Triplex and Quadruplex DNA Structures Studied by Electrospray Mass Spectrometry

Frédéric ROSU[1],Valérie GABELICA[2,*], Claude HOUSSIER[1], Pierre Colson[1],

Edwin DE PAUW[2]

1. Laboratoire de Biospectroscopie, Institut de Chimie (Bat. B6c), Université de Liège, B-4000 Liège, Belgium..
2. Laboratoire de Spectrométrie de Masse, Institut de Chimie (Bat. B6c), Université de Liège, B-4000 Liège, Belgium

* Address correspondence to: V. Gabelica, Mass Spectrometry Laboratory, Institut de Chimie (Bat. B6c), Université de Liège, B-4000 Liège, Belgium. Fax. 32-4-3663413. e-mail : v.gabelica@ulg.ac.be

Abstract

DNA triplex and quadruplex structures have been successfully detected by electrospray mass spectrometry. Circular dichroism and UV-melting experiments show that these structures are stable in 150 mM ammonium acetate at pH = 7 for the quadruplexes and pH = 5.5 for the triplexes. The studied quadruplexes were the tetramer $[d(TGGGGT)]_4$, the dimer $[d(GGGGTTTTGGGG)]_2$, and the intramolecular folded strand $dGGG(TTAGGG)_3$, which is an analog for the human telomeric sequence. The absence of sodium contamination allowed demonstration of the specific inclusion of *n*-1 ammonium cations in the quadruplex structures, *n* being the number of consecutive G-tetrads. We also detected the complexes between the quadruplexes and the quadruplex-specific drug mesoporphyrin IX. MS/MS spectra of $[d(TGGGGT)]_4$ and the complex with the drug are also reported. As the drug does not displace the ammonium cations, one can conclude that the drug binds at the exterior of the tetrads, and not between them. For the triplex structure, the ESI-MS spectra show the detection of the specific triplex, at *m*/*z* values typically higher than those typically observed for duplex species. Upon MS/MS the antigene strand, which is bound into the major groove of the duplex, separates from the triplex. This is the same dissociation pathway as in solution. To our knowledge this is the first report of a triplex DNA structure by electrospray mass spectrometry.

Introduction

Nucleic acids are the target of many different kinds of small molecule drugs. For example, a very successful approach for the development of antitumor drugs is the targeting of double-stranded DNA in order, for example, to interfere with the replication process to stop cell proliferation[1,2]. Another kind of nucleic acid target is RNA. RNA can fold in very diverse tertiary structures, and is responsible for different functions in cells (and in particular, gene expression). It is also a validated drug target for antibacterial treatment[3]. Several review papers have described the hows and whys of the electrospray mass spectrometry technique for the investigation of noncovalent complexes[4-7], and its implications for drug discovery[8,9]. In particular, several groups have reported the study of noncovalent complexes of small molecules with double-stranded DNA[10-15] or with RNA[16-18]. Drug-nucleic acid interactions studied by ESI-MS have been reviewed recently[19,20].

The present paper is part of a research program which aims at developing the use of ESI-MS for the study of small molecule interactions with various DNA targets including double-stranded DNA, but also G-quadruplexes and triple helices[21-23]. The latter two structures are formed by hydrogen bonding interactions different from those in the Watson-Crick binding mode encountered in double-stranded B-DNA (see Figure 1). This first step, reported here, is the characterization of triplex and quadruplex targets by ESI-MS and the study of the experimental conditions (buffer, source conditions) that allow preservation of these DNA structures.

G-quadruplex structures are formed by the planar arrangement of four guanine bases, as shown in Figure 1(a). These structures are encountered at the ends of chromosomes, the telomeres. Telomeres are a repeat of guanine-rich sequences that have several functions essential for genome integrity. The human telomeric repeat is (TTAGGG), and the extreme

terminal part of the telomeric DNA can form an intramolecular quadruplex structure. Telomerase, a reverse transcriptase enzyme, adds guanine-rich repeats to the ends of chromosomes to preserve the telomere length. Telomerase and telomeres are the focus of a great number of studies as a result of the implications of telomere-length regulation for cell immortality and cancer.[24,25] Since it has been shown that G-quartet structures inhibit telomerase in the protozoan *Oxythicha*[26], G-quadruplex structures have become attractive targets in cancer research[27]. There is therefore an active search for drugs that would stabilize the folded conformation of the telomeres, which inhibits telomerase activity.

G-quadruplex structures have been investigated by NMR spectroscopy and X-ray crystallography. Different studies have demonstrated that G-quadruplexes are stabilized by atomic cations placed between tetrads[28], as shown schematically in Figure 1b. G-quadruplexes could be detected in the presence of Na^+, K^+, but also NH_4^+[29-33]. The latter cation is the most interesting for its suitability for mass spectrometric studies, and we will demonstrate by solution studies and by ESI-MS that the quadruplex structures are conserved in ammonium acetate buffer. Several papers already reported the observation of quadruplex structures by ESI-MS. Goodlett et al.[34] reported the observation of the tetramer $[d(CGCGGGGGCG)]_4$ in a sodiated solution. Two other papers[35,36] report the association of guanines, guanine monophosphates or their derivatives, with alkali ions which form defined stoichiometries indicative of a 4-fold symmetry. Very recently, the interaction of the quadruplex $[d(TTGGGGGT)]_4$ with drugs, studied by ESI-MS, was reported[37]. In the present paper we report the study of three different quadruplexes (Q1, Q2 and Q3). Q1 = $[d(TGGGGT)]_4$ (Fig. 1b) is a tetramer which serves as a control, because the mass of the tetramer unambiguously demonstrates the presence of a quadruplex; Q2 = $[d(GGGGTTTTGGGG)]_2$ (Fig. 1c) is a dimer analogous to the telomeric repeat of *Oxytricha*; and Q3 = $d((GGG(TTAGGG)_3)$ (Fig. 1d) is an intramolecular folded quadruplex mimicking the human telomere.

In a triple helical DNA (or triplex), a single-strand oligonucleotide binds into the major groove of a double helix. The hydrogen bonding interactions between the bases of the third strand and those of the duplex are referred to as Hoogsteen or Hoogsteen-like hydrogen bonds (Figure 1e)[38]. DNA triplex formation offers an elegant approach for targeting double-stranded DNA (antigene approach) or RNA (antisense approach) with extensive sequence recognition[39]. Here we report the detection of a DNA triplex (an antigene strand bound to a B-DNA duplex). The stability of a triple-helix is usually less than that of double stranded DNA structures under physiological conditions. This is due, in part, to the electrostatic repulsion between the third strand and the duplex (an acidic pH is necessary to protonate the cytosines of the third strand[38,40]). There is also an active search for drugs that would stabilize triplex structures[41,42]. To our knowledge, this is the first report on the observation of triplex DNA by electrospray mass spectrometry.

Experimental section

Materials

All Single stranded oligodeoxyribonucleotides were purchased from Eurogentec (Angleur, Belgium). Quadruplex solutions were prepared in 150 mM NH_4OAc (pH = 7.0) with the strands d(TGGGGT) (M = 1863.26 Da), d(GGGGTTTTGGGG) (M = 3788.50 Da) and d(GGG(TTAGGG)$_3$) (M = 6653.35 Da) for quadruplexes Q1, Q2 and Q3 respectively. To avoid sodium contamination as far as possible, all stock solutions, including the solvents, were stored in polypropylene tubes. The oligonucleotides were used as received, without further desalting. The triplex was formed from the single strands d(CCTTTTCTCTTTCC) (M = 4106.71 Da), and d(GGAAAGAGAAAAGG) (M = 4418.96 Da), which constitute a Watson-Crick duplex, and the strand d(CCTTTCTCTTTTCC) (M = 4106.71 Da), which is the antigene strand. The triple helix solution was prepared in 150 mM NH_4OAc acidified by acetic acid (pH = 5.5). A minimum of 150 mM ammonium acetate is necessary to observe the triplex and an acidic pH helps to reduce the charge density of the third strand by protonation of the cytosine base to promote the formation of the C^+*GC base triplet. Sodium contamination was observed in the spectra of the triplexes, probably because of the large number of phosphate groups present. For the triplexes, sodium contamination is less critical for the discussion (see below). Solutions were heated to 80 °C and cooled overnight to form the quadruplexes or triplexes.

CD spectroscopy

CD spectra were recorded using a Jobin Yvon CD6 spectropolarimeter using 1-cm pathlength cell at 20 °C. The CD spectrum of each sample is the average of four scans. The spectral contribution of ammonium acetate was subtracted using the software supplied with the spectrometer.

Thermal denaturation

Thermal denaturations were performed using a UV spectrophotometer Lambda 5 (Perkin Elmer, Norwalk, CT, USA) interfaced with a PC XT for data acquisition. The quartz cells were heated with a Julabo F25 heating circulator (Kutztown, PA, USA).

Mass Spectrometry

For the quadruplexes, two different instruments were used: an LCQ ion trap instrument (ThermoQuest, San Jose, CA), equipped with its standard heated capillary electrospray source, and a Q-TOF2 instrument (Micromass, Manchester, UK), equipped with a Z-spray source. Both were operated in the negative ion mode. To obtain a stable electrospray signal, it was necessary to add 15% methanol just before injection. Unless mentioned explicitly in the text, the source conditions were as follows. For the LCQ, the heated capillary temperature was set to 180 °C, the tube lens offset was set to 35 V and the voltage on the heated capillary to –10 V (the skimmer is at ground). Collisional activation was also minimized in the octapoles. Full scan mass spectra were recorded in the m/z range [600-2000], and 50 scans were summed for each spectrum. For the Q-TOF2 instrument, the experimental conditions were optimized as follows: for the Z-Spray, a source block temperature of 70 °C, a desolvation temperature of 90 °C, a cone voltage of 20 V, and a collision energy of 10 eV were used.

For the triplex, the Q-TOF2 instrument was preferred, both for its larger mass range, and for the more adequate desolvation that could be achieved. A source block temperature of 70 °C, a desolvation temperature of 100 °C, a cone voltage of 40 V, and a collision energy of 10 eV were used.

Results and Discussion

G-Quadruplex DNA

CD and UV monitoring of melting in ammonium acetate

UV-melting experiments were performed to probe the stability of the quadruplex structures in solution. We have recorded the absorbance spectra at 260 nm and 295 nm in parallel for the quadruplexes as a function of temperature (raw data not show). DNA denaturation (for duplexes, triplexes and quadruplexes) is always characterized by a hyperchromism at 260 nm upon increasing the temperature. Table 1 summarizes the values of the melting temperatures obtained for the studied quadruplexes at 260 nm. The telomeric intramolecular quadruplex Q3 is the most stable in solution, but all three quadruplexes are stable at 20 °C in 150 mM NH_4OAc. At 295 nm, however, it has been shown[45] that a decrease of the absorbance upon increasing the temperature is specific to the dissociation of G-quartet structures. All melting profiles obtained were sigmoidal and the hypochromism observed at 295 nm upon denaturation confirmed that a quadruplex structure was present (data not shown). The melting temperatures obtained at 295 nm were similar to those obtained at 260 nm.

Circular dichroism (CD) was used to characterize the solution conformation of the studied quadruplexes in ammonium acetate. The CD data allow establishing consistent assignments for parallel and antiparallel quadruplex DNA. This nomenclature refers to the relative orientation (5' $\rightarrow$ 3') of the strands in the quadruplex. A parallel quadruplex has a maximum near 265 nm and a minimum near 240 nm. An antiparallel quadruplex is characterized by a maximum near 290 nm and a minimum near 260 nm[33,46]. Previous studies have demonstrated that NH_4^+ cations have a stabilizing effect on a G-tetrad[29-33]. Ammonium cations (^{15}N labeled)

are even used as probes of quadruplex formation. Nuclear overhauser effects (NOEs) observed between the NH_4^+ ion and guanine imino- protons show that ammonium ions are located between adjacent G-quartets[43].

We have performed CD experiments to characterize the quadruplex formation in 150 mM ammonium acetate at 20 °C. Figure 2 shows the CD spectra of the three quadruplexes. Quadruplex Q1 (Fig. 2a) is a parallel quadruplex in NH_4OAc. For quadruplexes Q2 and Q3 (Fig. 2b and 2c), the CD spectra indicate an antiparallel conformation. For the human telomeric sequence Q3, the same CD spectrum is observed in NaCl and KCl[47]. Plausible structures are represented in Figures 1 b, c and d for quadruplexes Q1, Q2 and Q3, respectively. The position of the ammonium cations between the tetrads is represented schematically in Fig. 1b.

ESI-MS

The ESI-MS spectrum of Q1 shows the tetramer in two charge states (Figure 3). The peaks at m/z 1499.7 and 1875 correspond to the four-stranded structure $(TGGGGT)_4$ with specifically 3 ammonium adducts, at charge states 5- and 4-, respectively. The species $[(TGGGGT)_4 + 3NH_4 - 7H]^{4-}$ (m/z = 1875) can be distinguished easily from the species $[TGGGGT]^-$ (m/z = 1862). There is no significant signal contribution from sodium adducts. It has been demonstrated by molecular modeling studies[48,49] that G-quadruplexes are very stable and rigid structures, and that the cations inside the structure between two adjacent tetrads play a role to stabilize the molecule. Some single strands with 1 or 2 negative charges are also observed. In the electrospray source conditions used for duplex DNA detection, no ammonium adducts are usually formed, due to the facile loss of neutral NH_3. For the quadruplex Q1, the fact that the complex is selectively detected with 3 ammonium ions indicates that these three ions are

bound very tightly to the quadruplex. They would be readily lost if they were nonspecifically attached to the DNA phosphate groups.

The ESI-MS spectra of the quadruplexes Q2 and Q3 are shown in Figure 4. For Q2, the most intense peak corresponds to $(GGGGTTTTGGGG)_2^{5-}$. As this strand cannot form a Watson-Crick self-complementary duplex, it is highly probable that the dimer is formed due to a G-quadruplex motif like that illustrated in Fig. 1c. For the quadruplex Q3, only the single-stranded form is detected. It is impossible at this stage to assess whether it is in an intramolecular folded G-quadruplex conformation or in an unfolded conformation.

Because it was shown that for Q1 there are clearly three ammonium cations in the quadruplex, we expected to observe (*n*-1) ammonium adducts for all quadruplexes, *n* being the number of consecutive G-tetrads. Figure 5 (a-d) shows enlargements of the 5- charge state peak of quadruplex Q2 for different source conditions. It is clear that Q2 needs much softer source conditions than Q1 in order to avoid the loss of the ammonium adducts. Nevertheless, it is possible to observe the Q2 quadruplex with specifically 3 ammonium adducts (n = 4) in very soft conditions. In the Q-TOF2, these conditions were achieved by lowering the cone voltage to 15 V and the collision energy in the MS mode to 6 eV (as opposed to the standard 10 eV recommended by the manufacturer). In the LCQ, suitably soft conditions were attained with a low capillary temperature (110 °C), a low capillary voltage (-8 V) and a tube lens offset of +35 V. The spectra recorded using the Q-TOF2 and the LCQ look very similar. For the quadruplex Q3, Figure 5 (e-h) shows the effect of the capillary temperature of the LCQ on the adducts. The lower the temperature, the larger the amount of adducts, but no specific stoichiometry is noticeable. This indicates that, if any ammonium is occluded in the G-tetrads, it is as easily removed in the gas phase as nonspecific adducts on the phosphate groups.

The comparison between Q1, Q2 and Q3 shows that the stability of the ammonium cations in the tetrads depends on the conformational strains induced by the loops of the quadruplex. Q1

is a tetramer that has no loop and the specific ammonium adducts are very stable; Q2 is a dimer that has two loops and the specific adducts could be detected only in very soft conditions; Q3 is an intramolecular folded-back structure with three loops and no specific ammonium adducts could be detected. It is worth mentioning here that the inclusion of ions between the tetrads of an intramolecular tetraplex has never been evidenced by solution methods either, to our knowledge.

Specific drug binding

Based on the stoichiometry and on the ammonium adducts, it is still impossible to assess whether Q3 has a folded or unfolded conformation in the gas phase. We therefore studied the complexation of the quadruplexes with mesoporphyrin IX (MP, see structure in Figure 6). MP shows a weak but very specific binding to quadruplex structures compared to single-stranded, duplex or triplex DNA[50,51]. Figure 7 shows the ESI-MS spectra of a mixture of MP (10 µM) and each quadruplex (5 µM). 1:1 and 2:1 complex stoichiometries could be detected. In the same experimental conditions, no complex was observed with double-stranded DNA of various sequences (data not shown). The observation of 2:1 stoichiometry with Q2 and Q3 is not anomalous. The most common binding modes with quadruplexes are intercalation between the G-tetrads, external stacking, and groove binding. Some recent studies on cationic porphyrin interaction with quadruplexes[52,53] have shown that multiple stoichiometries are plausible, and that the drug could interact with the quadruplex either by intercalation between the tetrads or by end-stacking (at the top of the group of tetrads). Mass spectrometry also provides information on the binding mode. With Q1, the peaks of the observed complexes correspond to $[(TGGGGT)_4 + MP + 3NH_4 - nH]^{(n-3)-}$. As the three ammonium ions are kept in the complex, this may indicate that the drug is not stacked between the tetrads. However it can not be excluded that the ammonium cations could coordinate in the center of the

mesoporphyrin, which itself could stack between the tetrads. This issue was resolved by MS/MS (see below).

ESI-MS/MS

Figure 8 shows the MS/MS spectra of (a) $[(TGGGGT)_4 + 3\ NH_4 - 8H]^{5-}$ and (b) $[(TGGGGT)_4 + MP + 3\ NH_4 - 8H]^{5-}$ obtained using the LCQ at an activation time of 30 ms and activation amplitude of 15 %. The quadruplex in (a) loses the ammonium ions, and dissociates by losing a single strand with 2 negative charges (m/z = 930.1). The resulting triple-stranded species at m/z 1860.2 retains the 3 remaining negative charges. This peak can be assigned unambiguously because of the observed depurination (loss of guanine) from $[(TGGGGT)_3]^{3-}$. At lower activation amplitude and longer reaction times, the loss of the ammonium ions is the predominant fragmentation pathway (data not shown), and this is therefore the lowest energy pathway.

Upon collisional activation of the complex of Q1 with MP (Fig. 8b), the drug leaves the quadruplex structure either with one negative charge or as a neutral. The intact corresponding quadruplex with its three specific ammonium ions is observed at the charge states 4- and 5- . Some single-stranded $TGGGGT^{2-}$ and triple-stranded $[(TGGGGT)_3]^{3-}$ can also be detected. These originate from the subsequent dissociation of the quadruplex Q1 (see Fig. 8a). A similar behavior was reported by David et al.[37] for the dissociation of a complex between Tel01, a drug that stacks at the ends of the tetrads, and a quadruplex. This article[37], however, reports the MS/MS of a sodiated complex. The present MS/MS were performed MS/MS on the complex with its three specific ammonium cations. The fact that the drug is expelled from the duplex before NH_3 is a better indication that the drug is not stacked between the tetrads, but is bound outside. David et al.[37] also found that, in contrast with the end-stacking drug Tel01, groove binders did remain attached to the strands upon dissociation. Nevertheless, care should be taken not to draw hasty conclusions on the binding mode from the MS/MS

dissociation pathways alone. In particular, groove binders are usually positively charged molecules, while drugs that are capable of stacking with DNA bases are usually neutral. It has not been demonstrated to date whether the MS/MS dissociation pathway is conditioned by the binding mode, by the charge of the drug, or both.

Triplex DNA

UV-melting in ammonium acetate

The stability of the triple helical structure was monitored in ammonium acetate (150 mM) acidified with acetic acid (pH = 5.5). The change in UV absorbance at 260 nm was followed as a function of temperature (Figure 9). The biphasic profile obtained is characteristic of the triple helical denaturation [41]. The first transition at low temperature (Tm = 35 °C) corresponds to the separation of the antigene strand from the duplex (triplex $\rightarrow$ duplex + antigene). At higher temperatures, the dissociation of the duplex appears (Tm = 58 °C) (duplex $\rightarrow$ single strands transition). The triplex is therefore sufficiently stable at room temperature with our sample preparation.

ESI-MS

The observation by ESI-MS of a triple helix DNA structure was possible due to carefully chosen source conditions and appropriate solution medium. In particular, it was found that the Q-TOF2 instrument was more convenient than the LCQ to observe the triplex species. These appear at mass-to-charge ratios typically higher than duplexes, and harsher source conditions are needed to desolvate triplexes. The ESI-MS spectrum is shown in Figure 10. The triple helical structure appears at charge states 7- (m/z = 1803.5) and 6- (m/z = 2104.3). The charge

states could be assigned from the *m*/*z* spacing between the multiple sodium adducts. The peak at *m*/*z* = 1704.1 corresponds the 14-mer duplex with 5 negative charges, which can be in slight excess compared to the antigene single strand.

ESI-MS/MS

MS/MS was conducted on the $[Triplex]^{7-}$ species, and the spectrum is shown in Figure 11. The triplex fragments via the following pathway: $Triplex^{7-} \rightarrow Duplex^{4-} + Antigene^{3-}$. This is similar to the dissociation pathway encountered in solution (see Fig. 9): the antigene strand that is bound in the major groove of the double helix is expelled first.

Conclusion

In summary, we have shown that triplex and quadruplex DNA structures can be easily studied by electrospray mass spectrometry in ammonium acetate electrolyte. For quadruplexes in particular, the absence of sodium contamination allowed demonstration of the conservation of specific ammonium cations inside the quadruplex structure. The detection of triplexes, quadruplexes, and complexes with drugs, in easy-to-handle experimental conditions, is very promising for the use of ESI-MS and MS/MS for the study of drug interactions with various DNA targets, and such studies are currently under way in our laboratory.

Acknowledgement

VG is grateful to the F.N.R.S. (Fonds National de la Recherche Scientifique) for a research fellowship.

References

1. Dervan PB. *Science* 1986; **232**: 64.

2. Pindur J, Fischer G. *Curr. Med. Chem.* 1996; **3**: 379.

3. Gallego J, Varani G. *Acc. Chem. Res.* 2001; **34**: 836.

4. Smith RD, Bruce JE, Wu Q, Lei QP. *Chem. Soc. Rev.* 1997; **26**: 191.

5. Loo JA. *Mass Spectrom. Rev.* 1997; **16**: 1.

6. Schalley CA. *Mass Spectrom. Rev.* 2001; **20**: 253.

7. Daniel JM, Friess SD, Rajagopalan S, Wendt S, Zenobi R. *Int. J. Mass Spectrom.* 2002; **216**: 1.

8. Loo JA, Dejohn DE, Du P, Stevenson TL, Ogorzalek Loo RR. *Med. Res. Rev* 1999; **19**: 307.

9. Siegel MM. *Curr. Top. Med. Chem.* 2002; **2**: 13.

10. Gale DC, Smith RD. *J. Am. Soc. Mass Spectrom.* 1995; **6**: 1154.

11. Triolo A, Arcamone FM, Raffaelli A, Salvadori P. *J. Mass Spectrom.* 1997; **32**: 1186.

12. Gabelica V, De Pauw E, Rosu F. *J. Mass Spectrom.* 1999; **32**: 1328.

13. Kapur A, Beck JL, Sheil MM. *Rapid Commun. Mass Spectrom.* 1999; **13**: 2489.

14. Wan KX, Shibue T, Gross ML. *J. Am. Chem. Soc.* 2000; **122**: 300.

15. Reyzer M, Brodbelt JS, Kerwin SM, Kumar D. *Nucleic Acids Res.* 2002; **29**: e103.

16. Hofstadler SA, Sannes-Lowery KA, Crooke ST, Ecker DJ, Sasmor H, Manalili S, Griffey RH. *Anal. Chem.* 1999; **71**: 3436.

17. Griffey RH, Sannes-Lowery KA, Drader JJ, Mohan V, Swayze EE, Hofstadler SA. *J. Am. Chem. Soc.* 2000; **122**: 9933.

18. Sannes-Lowery KA, Griffey RH, Hofstadler SA. *Anal. Biochem.* 2000; **280**: 264.

19. Beck J, Colgrave ML, Ralph SF, Sheil MM. *Mass Spectrom. Rev.* 2001; **20**: 61.

20. Hofstadler SA, Griffey RH. *Chem. Rev.* 2001; **101**: 377.

21. Shafer RH. *Prog. Nucl. Acid Res. Mol. Biol.* 1998; **5**: 55.

22. Jenkins TC. *Curr. Med. Chem.* 2000; **7**: 99.

23. Belmont P, Constant J-F, Demeunynk M. *Chem. Soc. Rev.* 2001; **30**: 70.

24. Collins K. *Curr. Opin. Cell Biol.* 2000; **12**: 378.

25. Lavelle F, Riou J-F, Laoui A, Mailliet P. *Crit. Rev. Oncol. Hematol.* 2000; **34**: 111.

26. Zahler AM, Williamson JR, Cech TR, Prescott DM. *Nature* 1991; **350**: 718.

27. Mergny J-L, Mailliet P, Lavelle F, Riou J-F, Laoui A, Hélène C. *Anti-cancer Drug Design* 1999; **14**: 327.

28. Williamson JR. *Annu. Rev. Biophys. Biomol. Struct.* 1994; **23**: 703.

29. Nagesh N, Chatterji D. *J. Biochem. Biophys. Methods* 1995; **30**: 1.

30. Guschlbauer W, Chantot J-F, Thiele D. *J. Biomol. Struct. Dyn.* 1990; **8**: 491.

31. Rovnyak D, Baldus M, Wu G, Hud NV, Feigon J, Griffin RG. *J. Am. Chem. Soc.* 2000; **122**: 11423.

32. Schultze P, Hud NV, Smith FW, Feigon J. *Nucleic Acids Res.* 1999; **27**: 3018.

33. Giraldo R, Suzuki M, Chapman L, Rhodes D. *Proc. Natl. Acad. Sci. USA* 1994; **91**: 7658.

34. Goodlett DR, Camp DG, II, Hardin CC, Corregan M, Smith RD. *Biol. Mass Spectrom.* 1993; **22**: 181.

35. Fukushima K, Iwahashi H. *Chem. Commun.* 2000; 895.

36. Manet I, Francini L, Masiero S, Pieraccini S, Spada GP, Gottarelli G. *Helv. Chim. Acta* 2001; **84**: 2096.

37. David WM, Brodbelt J, Kerwin SM, Thomas PW. *Anal. Chem.* 2002; **74**: 2029.

38. Plum GE, Pilch DS, Singleton SF, Breslauer KJ. *Annu. Rev. Biophys. Biomol. Struct.* 1995; **24**: 319.

39. Hélène C. *Anti-cancer Drug Design* 1991; **6**: 569.

40. Gowers DM, Fox KR. *Nucleic Acids Res.* 1999; **27**: 1569.

41. Mergny J-L, Duval-Valentin G, Nguyen CH, Perrouault L, Faucon B, Rougée M, Montenay-Garestier T, Bisagni E, Hélène C. *Science* 1992; **256**: 1681.

42. Escudé C, Nguyen CH, Kukreti S, Janin Y, Sun J-S, Bisagni E, Garestier T, Hélène C. *Proc. Natl. Acad. Sci. USA* 1998; **95**: 3591.

43. Hud NV, Schultze P, Sklenar V, Feigon J. *J. Mol. Biol.* 1999; **285**: 233.

44. Wang Y, Patel DJ. *Structure* 1993; **1**: 263.

45. Mergny J-L, Phan A-T, Lacroix L. *FEBS Lett.* 1998; **435**: 74.

46. Lu M, Guo Q, Kallenbach NR. *Biochemistry* 1993; **32**: 598.

47. Balagurumoorthy P, Brahmachari SK. *J. Biol. Chem.* 1994; **269**: 21 858-21 869.

48. Spackova N, Berger I, Sponer J. *J. Am. Chem. Soc.* 1999; **121**: 5519.

49. Chowdhury S, Bansal M. *J. Biomol. Struct. Dyn.* 2000; **17**: 11.

50. Ren J, Chaires JB. *Biochemistry* 1999; 16067.

51. Arthanari H, Basu S, Kawano TL, Bolton PH. *Nucleic Acids Res.* 1998; **26**: 3724.

52. Han FX, Wheelhouse RT, Hurley LH. *J. Am. Chem. Soc.* 1999; **121**: 3561.

53. Han H, Langley DR, Rangan A, Hurley LH. *J. Am. Chem. Soc.* 2001; **123**: 8902.

54. Versluis C, Heck AJR. *Int. J. Mass Spectrom.* 2001; **210/211**: 637.

55. Felitsyn N, Kitova EN, Klassen JS. *Anal. Chem.* 2001; **73**: 4647.

Table

Table 1. Melting temperatures of the quadruplexes (3.5 μM) in 150 mM NH_4OAc.

	Sequence	Tm (°C)
Q1:	$[d(TGGGGT)]_4$	36
Q2:	$[d(GGGGTTTTGGGG)]_2$	56
Q3:	$d(GGG(TTAGGG)_3)$	58

Figure legends

Figure 1

(a) Schematic drawing of a G-quartet. (b) Schematic representation of the quadruplex structure Q1 = $[d(TGGGGT)]_4$ with the ammonium ions placed between the tetrads. (c) Schematic representation of the quadruplex structure Q2 = $[d(GGGGTTTTGGGG)]_2$, according to NOE experiments [43]. (d) Structure of the folded telomeric sequence $dGGG(TTAGGG)_3$. The structure has been drawn with Accelrys ViewerLite 4.2 with the PDB structure 143D, obtained by NMR [44]. (e) Hydrogen bonding in the parallel triplets T∗AT and C^+∗GC. (f) Schematic representation of a triplex structure.

Figure 2

CD spectra of quadruplexes Q1, Q2 and Q3 in 150 mM ammonium acetate (pH 7.0) at 20 °C. The quadruplex concentration was 4 µM in each case.

Figure 3

ESI-MS full scan spectrum of quadruplex Q1 in 150 mM ammonium acetate (pH 7.0). The spectrum was recorded using the LCQ.

Figure 4

ESI-MS full scan spectra of Q2 (top) and Q3 (bottom) in 150 mM ammonium acetate (pH 7.0). The spectra were recorded using the Q-TOF2.

Figure 5

(a-d) Enlargements of the distribution of ammonium adducts on quadruplexes Q2 recorded using the Q-TOF2 at different cone voltages (V_{cone}) and collision energies (CE): (a) V_{cone} = 15 V, CE = 6 eV; (b) V_{cone} = 15 V, CE = 8 eV; (c) V_{cone} = 15 V, CE = 10 eV; (d) V_{cone} = 20 V, CE = 10 eV. (e-h) Zooms of the distribution of ammonium adducts on quadruplexes Q3 recorded using the LCQ at different capillary temperatures: (e) T_{cap} = 110 °C; (f) T_{cap} = 125

°C; (g) T_{cap} = 150 °C; (h) T_{cap} = 180 °C. The numbers represent the number of ammonium adducts.

Figure 6

Structure of mesoporphyrin IX (566 Da).

Figure 7

ESI-MS spectra of mixtures of 10µM mesoporphyrin IX (MP) with the quadruplexes Q1 (top), Q2 (middle) and Q3 (bottom), each at a concentration of 5µM. Spectra were recorded using the LCQ.

Figure 8

ESI-MS-MS spectra of (a) $[(TGGGGT)_4 + 3\ NH_4 - 8H]^{5-}$ (m/z = 1499.7) and (b) $[(TGGGGT)_4 + MP + 3\ NH_4 - 8H]^{5-}$ (m/z = 1612.8) obtained using the LCQ at an activation time of 30 ms and activation amplitude of 15 %.

Figure 9

Denaturation profile obtained by UV absorption at 260 nm for the triplex in 150 mM ammonium acetate (pH 5.5).

Figure 10

ESI-MS spectrum of the triplex, recorded using the Q-TOF2 (V_{cone} = 40 V).

Figure 11

ESI-MS-MS scan spectra (Q-TOF2) of the triplex^{7-} (m/z = 1803.5) at a collision energy of 16 eV (V_{cone} = 40 V).

Figure 1 (preferably two-column width)

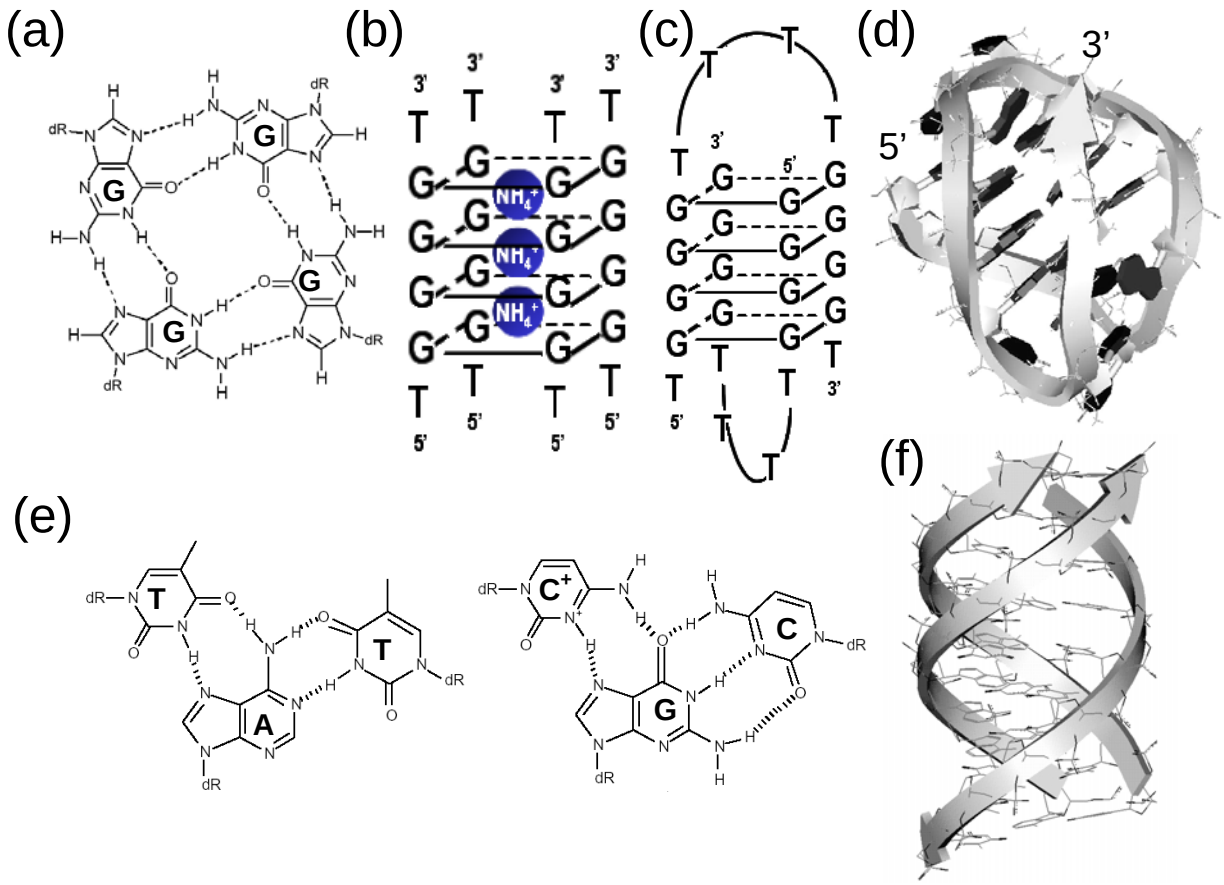

Figure 2

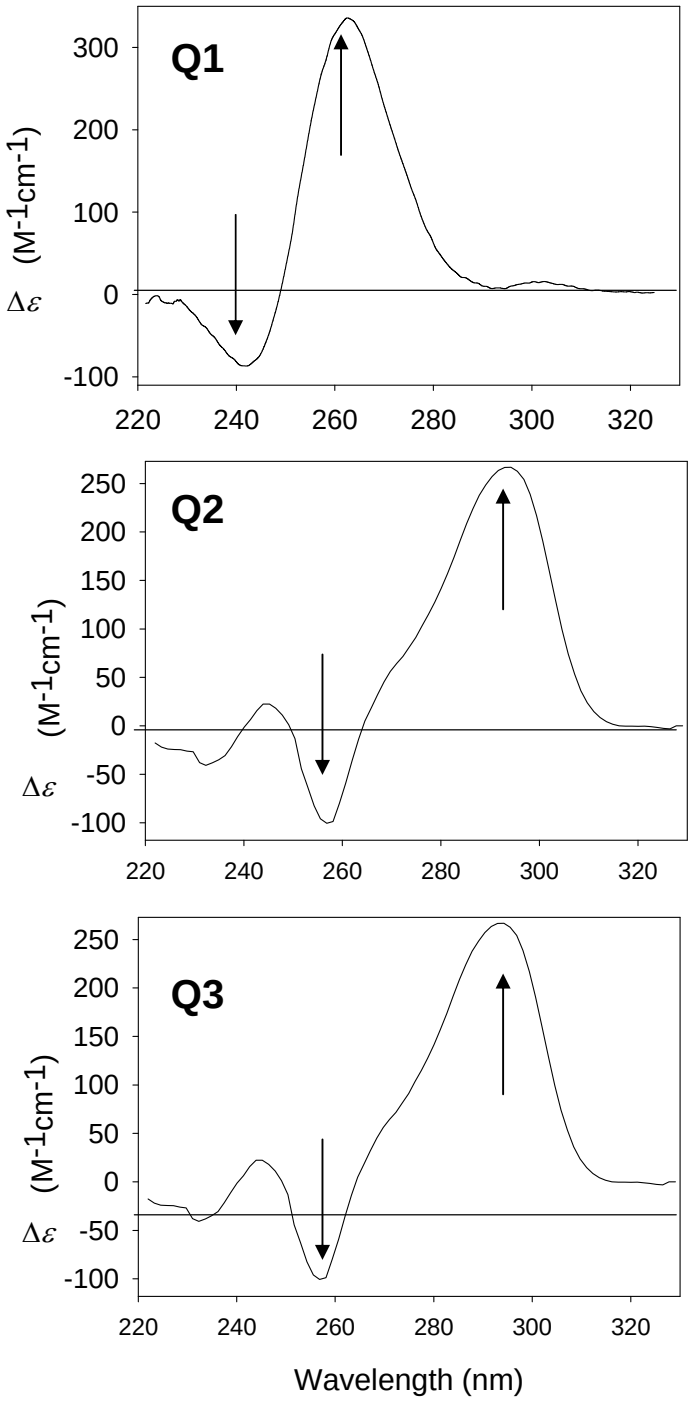
Q1
Q2
Q3
Δε (M-1cm-1)
300
200
100
0
-100
250
150
50
-50
220
240
260
280
300
320
Wavelength (nm)

Figure 3

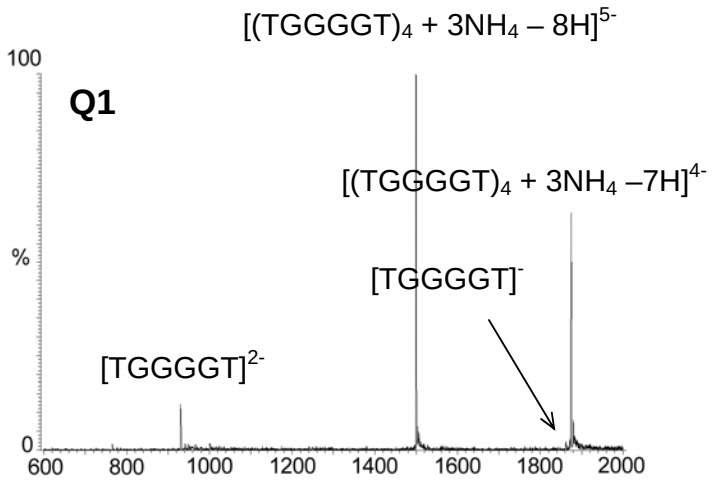
[(TGGGGT)4 + 3NH4 – 8H]5-
100
Q1
[(TGGGGT)4 + 3NH4 –7H]4-
%
[TGGGGT]-
[TGGGGT]2-
0
600
800
1000
1200
1400
1600
1800
2000

Figure 4

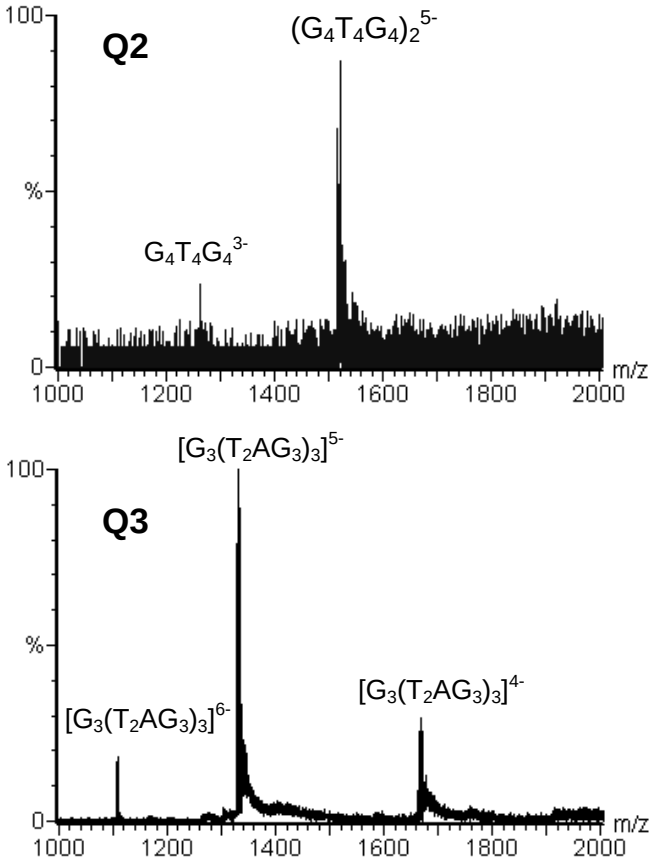
Q2
$(G_4T_4G_4)_2^{5-}$
$G_4T_4G_4^{3-}$
100
%
0
1000
1200
1400
1600
1800
2000
m/z
Q3
$[G_3(T_2AG_3)_3]^{5-}$
$[G_3(T_2AG_3)_3]^{6-}$
$[G_3(T_2AG_3)_3]^{4-}$
100
%
0
1000
1200
1400
1600
1800
2000
m/z

Figure 5

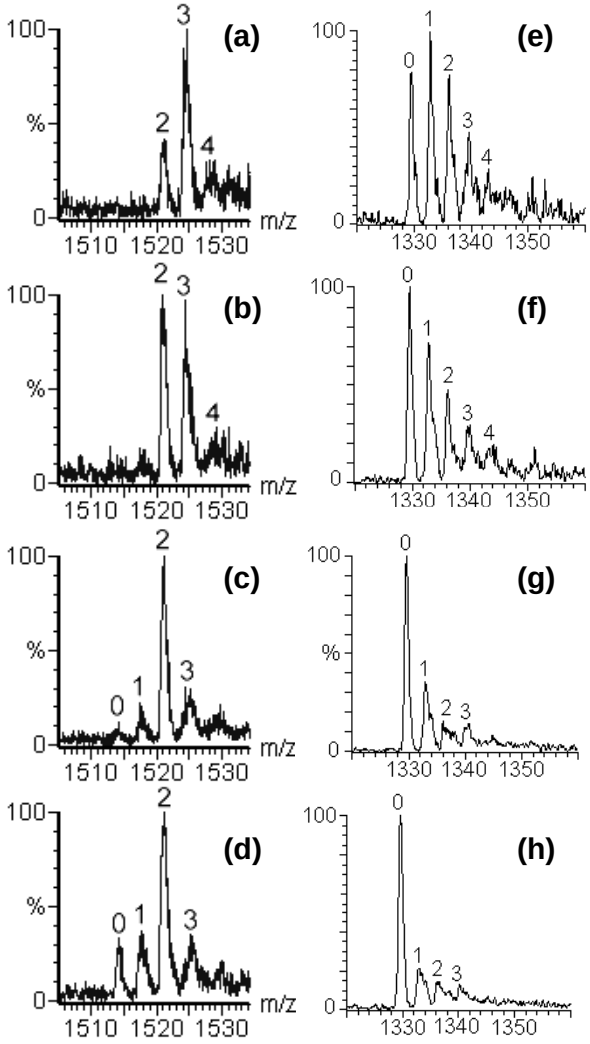

Figure 6

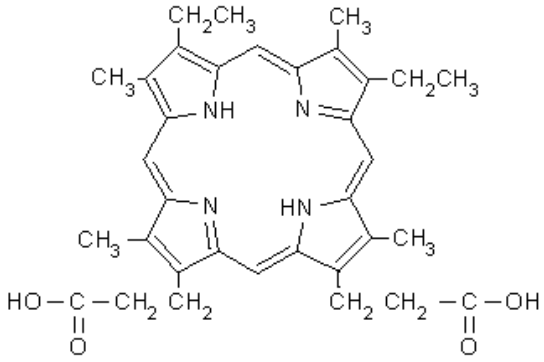
CH2CH3
CH3
CH3
CH2CH3
NH
N
N
HN
CH3
CH3
HO—C—CH2 CH2
O
CH2 CH2 —C—OH
O

Figure 7

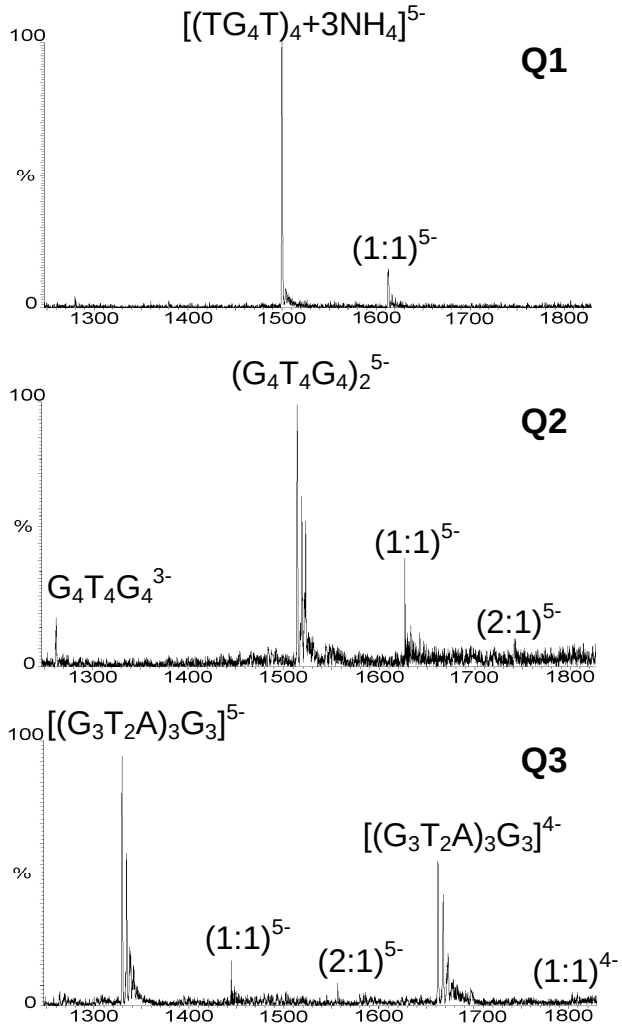
[(TG4T)4+3NH4]5-
Q1
100
%
0
(1:1)5-
1300
1400
1500
1600
1700
1800
(G4T4G4)25-
Q2
G4T4G43-
(1:1)5-
(2:1)5-
[(G3T2A)3G3]5-
Q3
[(G3T2A)3G3]4-
(1:1)5-
(2:1)5-
(1:1)4-

Figure 8

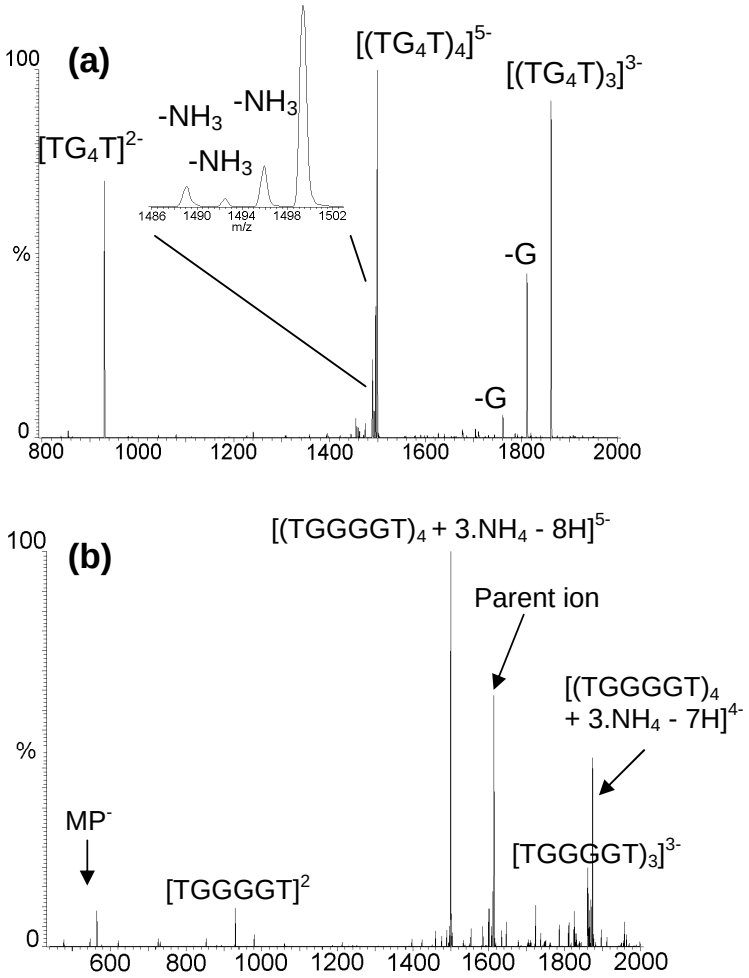
(a)
100
%
0
800
1000
1200
1400
1600
1800
2000
[TG4T]2-
-NH3
-NH3
-NH3
[(TG4T)4]5-
[(TG4T)3]3-
-G
-G
1486
1490
1494
1498
1502
m/z
(b)
[(TGGGGT)4 + 3.NH4 - 8H]5-
Parent ion
[(TGGGGT)4
+ 3.NH4 - 7H]4-
MP-
[TGGGGT]2
[TGGGGT)3]3-
600
800
1000
1200
1400
1600
1800
2000

Figure 9

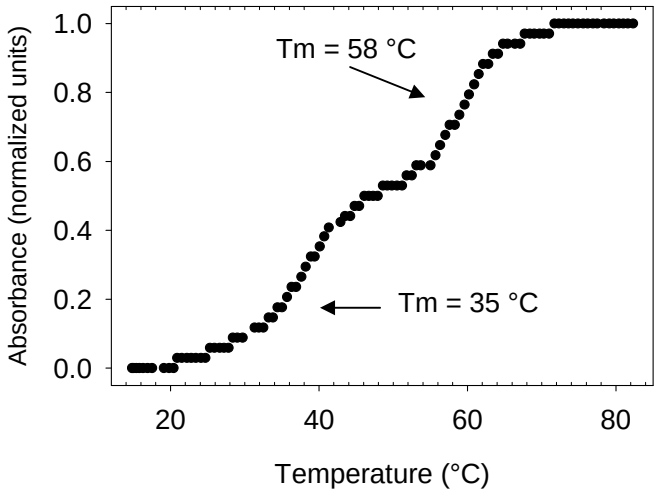
Absorbance (normalized units)
1.0
0.8
0.6
0.4
0.2
0.0
Tm = 58 °C
Tm = 35 °C
20
40
60
80
Temperature (°C)

Figure 10

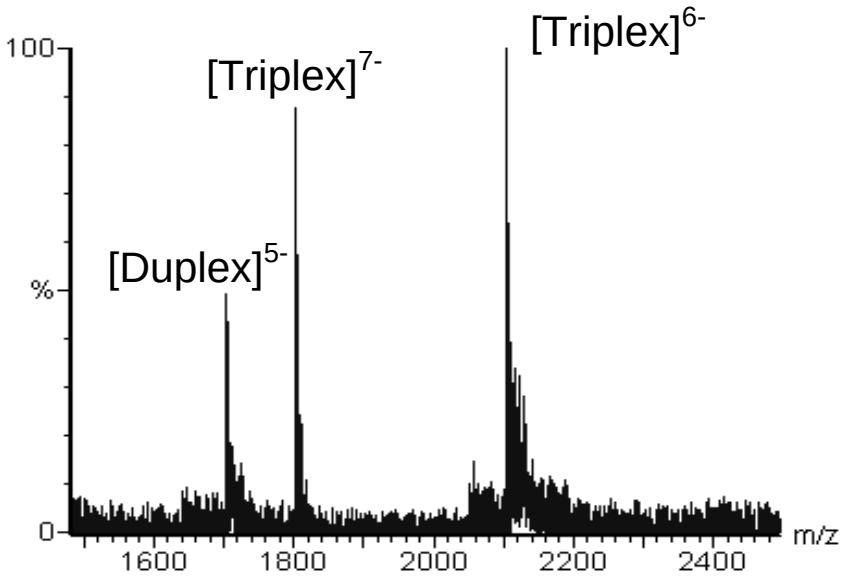

Figure 11